

A CASE EXAMPLE OF THE ROLE OF WARM-SECTOR  
CONVECTION IN THE DEVELOPMENT OF MESOSCALE  
BANDED SNOWFALL: 2003 NOVEMBER 22-24

Martin A. Baxter\*  
Central Michigan University  
Mt. Pleasant, MI

Charles E. Graves  
Saint Louis University  
St. Louis, MO

## 1. INTRODUCTION

Forecasting the presence, location, intensity, and duration of mesoscale snowbands remains one of the more difficult challenges during the winter season. These bands typically have a length to width ratio at or below the frontal scale; 5-50 km in width and 100-1000 km in length (Banacos 2003). Research on the physical processes that result in banded snowfall increasingly shows that the phenomenon of mesoscale snow banding cannot be associated with a ‘typical’ dynamic and thermodynamic atmospheric structure, but instead can arise from a variety of scenarios (e.g., Moore et al. 2005, Novak et al. 2004, Juriewicz and Evans 2004). In the analysis of a banded snow event, the relative roles of various physical processes and the synergistic interactions between them are analyzed to determine the characteristics of the snowfall. The mesoscale processes attendant with banded snowfall are largely controlled by large-scale airstreams known as conveyor belts. An example of the juxtaposition of the relevant physical processes in a banded snowfall event is shown in Fig. 1.

As the particulars of the mesoscale processes involved in banded snowfall can be related to the conveyor belts, it can be surmised that processes that impact the characteristics of these airstreams will have an impact on mesoscale snowfall production. Posselt and Martin (2004) demonstrated the strong influence latent heat release occurring in the trowal airstream has on the occlusion process. Indeed, many earlier studies have examined the effect convection has on the large scale, but only one to date has examined the effects of warm-sector convection on snowfall to the north of a warm frontal boundary (Brennan and Lackmann 2005). This work mimics the approach taken by Brennan and Lackmann (2005), but seeks to investigate the role of convection in direct relation to the balance of processes that cre-

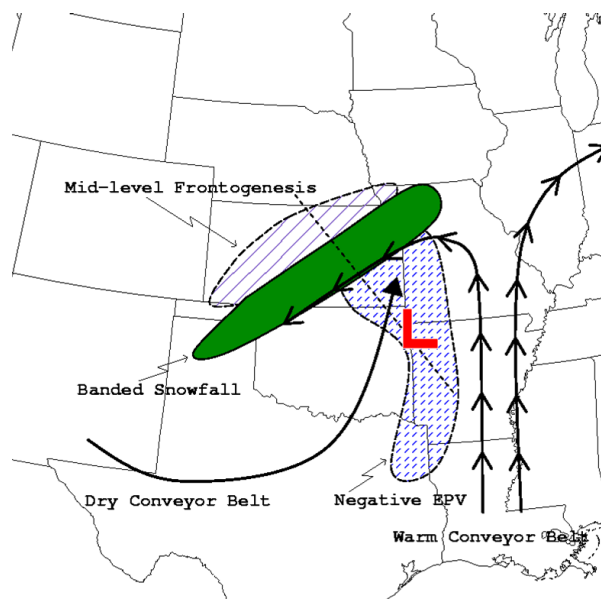


Figure 1: Conceptual model of physical processes (labeled in figure) contributing to heavy banded snow for the 4-5 December 1999 case. (Moore et al. 2005).

\* *Corresponding author address:* Martin A. Baxter, Dept. of Geography, Central Michigan University, Mt. Pleasant MI 48858; email: [baxtelma@cmich.edu](mailto:baxtelma@cmich.edu)

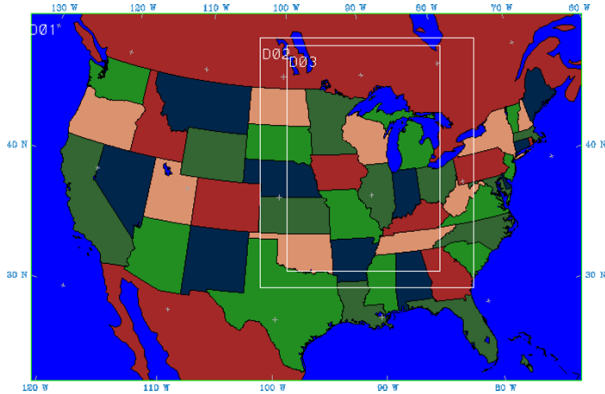


Figure 2: Model domain configuration for 22-24 November 2003 case.

ate banded snowfall. The fact that banded snowfall can exist with or without convection suggests that convection to the south of a region of banded snowfall may not always “steal” the moisture, an idea that anecdotal evidence suggests many operational forecasters hold true.

## 2. MODEL SIMULATION

Version 3.7 of the fifth-generation Pennsylvania State University-National Center for Atmospheric Research mesoscale model (MM5, Grell et al. (1995)) was used to simulate this event. A 48-h simulation was completed, spanning 1200 UTC 22 Nov 2003 through 1200 UTC 24 Nov 2003. Three two-way nested domains were used, with resolutions of 36 km, 12 km, and 4 km (Fig. 2). The innermost domain was defined to include both the banded snowfall and the convection. Vertical resolution consisted of 37 sigma levels. Parameterizations used were the Reisner 2 explicit microphysics scheme, the Grell cumulus parameterization scheme, the MRF planetary boundary layer scheme, the Dudhia cloud radiation scheme, and the five-layer soil model. No cumulus parameterization was used on the 4 km domain. Instantaneous temperature tendencies were output from the cumulus and explicit microphysics schemes. Trajectories were computed using version 4 of RIP (Read-Interpolate-Plot; Stoelinga (2005)).

Initial conditions and lateral boundary conditions were obtained from the North American Regional Reanalysis dataset. This data is archived every 3 hours, and contains 32 km horizontal resolution with 45 layers. The use of this dataset is advantageous, in that it contains similar resolution to the outermost grid and it allows the lateral boundary conditions to be updated more frequently than with Eta analysis

data.

## 3. SYNOPTIC OVERVIEW

This system featured a broad area of snowfall through South Dakota, Minnesota, and Wisconsin. Maximum snowfall of 10 to 12 in was reported, along with winds as high as 40 kts, leading to blizzard conditions (NCDC 2006). Convection occurred in the form of a quasi-linear convective system (QLCS) that developed in Missouri and propagated northward and eastward over time. Severe weather was reported with this convection, with thunderstorm winds of 70 kts and hail as large as 1 in (NCDC 2006).

This case featured fairly strong, slowly evolving upper level dynamics. At the initial time, zonal flow at 500 mb existed over much of the United States. A straight jet streak was present at 300 mb over Kansas and Nebraska, extending northeast through Minnesota and Wisconsin. A low-level thermal gradient is seen at the surface and 850 mb from Oklahoma northeast into Missouri, south of the upper-level jet streak. A developing surface low is present along the frontal boundary in the Texas panhandle. Through the remainder of the simulation, this low underwent cyclogenesis as the pattern at 500 mb became highly meridional with the approach of a strong shortwave trough and associated vorticity maximum. Further upper-level support for cyclogenesis was present in the form of a jet streak that developed on the eastward side of the shortwave trough. Simulated reflectivity at F2700 illustrates banded snowfall in Minnesota and Wisconsin, with a QLCS to the southeast (Fig. 3). The simulation was very accurate with respect to the large scale dynamics and the convective mode.

## 4. PV BUDGET

A PV budget was computed, using the methods provided by Raymond (1992) and Cammas et al. (1994), and used by Lackmann (2002) and Brennan and Lackmann (2005). The PV budget is useful in establishing that PV anomalies were generated in-situ via diabatic processes, rather than due to horizontal or vertical advection. Budget calculations were performed for F2100, four hours after the initiation of convection. Tendency terms are shown for 700 mb, with model-output diabatic heating shown for 650 mb, as it is known that PV anomalies develop beneath areas of maximum diabatic heating. Diabatic heating is concentrated along the axis of the QLCS, with a maximum value in excess of  $200 \times 10^{-5} \text{ K s}^{-1}$  in northern Missouri / west-central Illi-

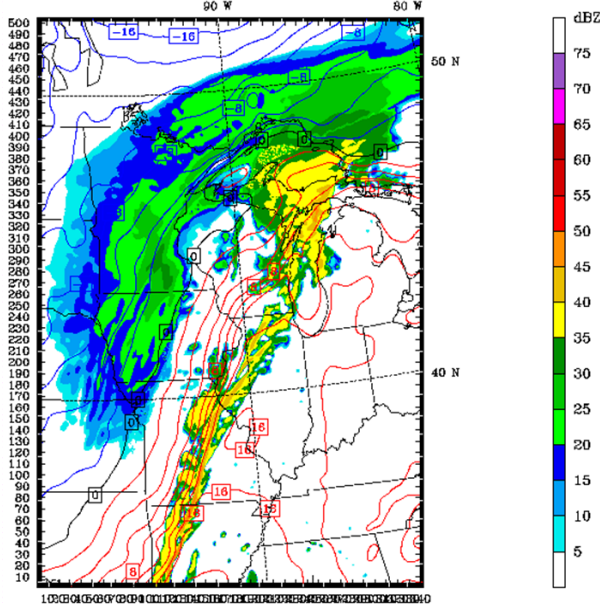


Figure 3: MM5 simulated reflectivity on domain three for 1500 UTC 23 Nov (F2700), in dBZ and surface temperature ( $2^{\circ}\text{C}$ , solid).

nois (Fig. 4a). A maximum in PV of 1.25-1.50 PVU (PVU = potential vorticity units =  $10^{-6} \text{ K m}^2 \text{ kg}^{-1} \text{ s}^{-1}$ ) is seen just north of the maximum diabatic heating, in southeastern Iowa. A secondary PV maximum is seen ahead of the QLCS in east-central Illinois. The nonadvective PV tendency provides the generation rate of PV due to diabatic processes (Fig. 4b). As expected, the nonadvective PV tendency is maximized along the QLCS, with a maximum value of 2 PVU  $3 \text{ hr}^{-1}$  in the aforementioned region of maximum diabatic heating. Positive values of nonadvective PV tendency are seen throughout the length of the QLCS, with additional positive values near the secondary PV maximum in eastern Illinois.

## 5. PV INVERSION

A nonlinear piecewise PV inversion based on the methodology devised by Davis and Emanuel (1991) was performed in order to quantify the impact of the diabatically produced PV on the flow and associated moisture transport. Mean state values of PV,  $\theta$ ,  $\phi$ ,  $\psi$  were computed from a 14-day MM5 simulation centered on the 48 hr primary simulation spanning the time period 0000 UTC 16 November 2003 through 0000 UTC 30 November 2003. F2700 was selected for inversion (see Fig. 3). The inversion was performed on a  $44 \times 56$  grid with a 36 km resolution.

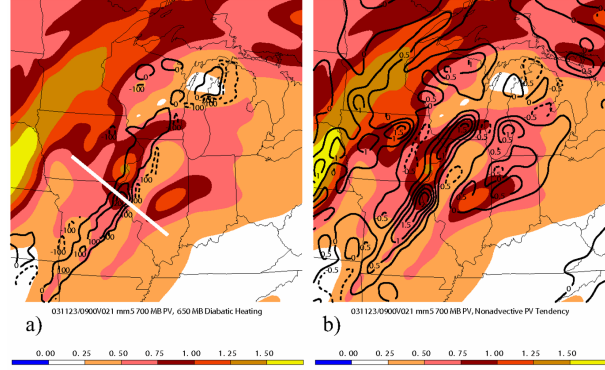


Figure 4: MM5 domain one (a) 700 mb PV (scale below; shaded) and 650 mb diabatic heating ( $100 \times 10^{-5} \text{ K s}^{-1}$ ; lines) and (b) 700 mb PV and nonadvective PV tendency ( $0.5 \text{ PVU } 3 \text{ hr}^{-1}$ ; lines) at 0900 UTC Nov 23 (F2100).

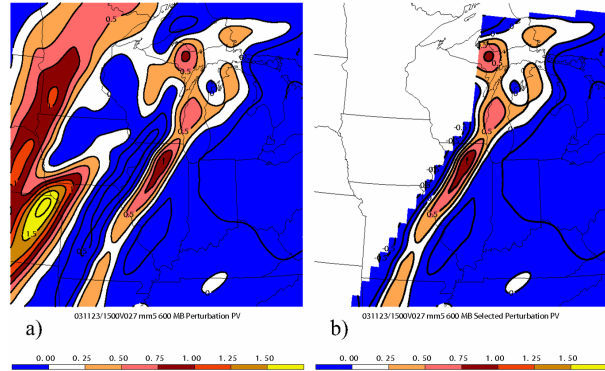


Figure 5: MM5 domain one (a) 600 mb perturbation PV (scale at bottom) and (b) 600 mb selected perturbation PV (scale at bottom). Valid for 1500 UTC 23 Nov (F2700).

Negative PV was set to a small positive value to ensure numerical convergence. 19 levels were used in the inversion, ranging from 1000 to 100 mb with an interval of 50 mb.  $\theta$  at 975 mb and 125 mb was used for the lower and upper boundary conditions, respectively.

Since F2100, the area of convection and associated PV has increased to the north, where it now takes on a less linear orientation (Fig. 5a). The perturbation PV is primarily vertically continuous in structure, though magnitudes differ depending on the level chosen. To examine the effects of the flow field of *only* the perturbation PV due to convection in the warm sector, a grid “mask” was created to isolate this PV (Fig. 5b). During the inversion, all

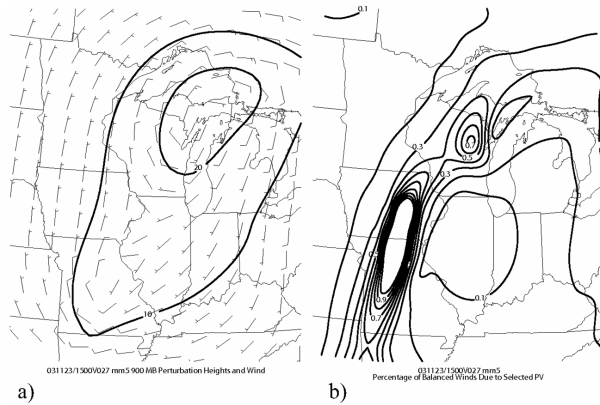


Figure 6: MM5 domain one (a) 900 mb perturbation heights (m) and winds (kts) and (b) percentage of balanced winds due to selected PV. Valid for 1500 UTC 23 Nov (F2700).

PV in the domain outside of that selected was set to zero. In addition, all anticyclonic (negative) perturbation PV was set to zero. Selected PV over a 900 to 500 mb layer was inverted.

The perturbation heights and winds at 900 mb resulting from the inversion of the selected PV are shown in Fig. 6a. Height falls of 20 m and an associated cyclonic circulation are observed near the eastern Upper Peninsula of Michigan. The wind field due to the inversion of the selected PV is compared to the wind field due to the full (1000-100 mb) inversion of all PV in Fig. 6b. The height and wind fields resulting from the selected PV must be viewed as a *contribution* to relevant physical processes, and not in terms of absolutes. Southerly winds over Lake Michigan contribute 20 to 30% of the total balanced flow, contributing to the northward transport of warm, moist, low-level air. North of Lake Superior, easterly winds also contribute 20 to 30% of the total balanced flow, enhancing the cold conveyor belt (CCB).

The height falls and cyclonic circulation are not in the vicinity of the primary surface low, which is further to the southwest. The selected PV produces a secondary surface low that arises due to diabatically produced PV within the northward advancing QLCS. This secondary low is seen within the model simulation. This feature is slightly more apparent at F3000 rather than F2700, thus this time is shown in Fig. 7a. At F2700, the observed surface map indicates a secondary surface low over Lake Michigan (Fig. 7b), a testament to the validity of the model simulation and its ability to represent diabatic processes and their impacts.

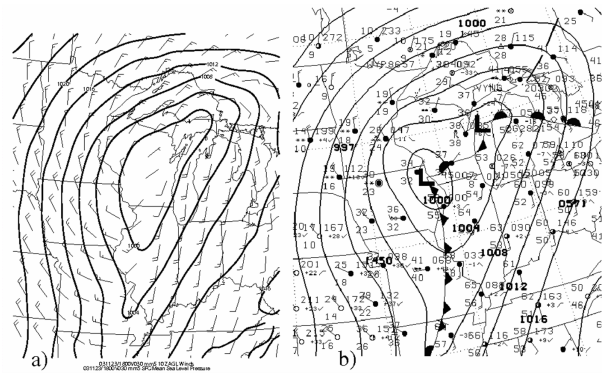


Figure 7: (a) MM5 domain one mean sea level pressure (solid, 4 mb), surface temperatures (dashed; 5°F), and winds in knots at 1800 UTC 23 Nov (F3000). (b) NCEP surface analysis for 1500 UTC 23 Nov (F2700).

## 6. TRAJECTORY ANALYSIS

Trajectory analysis was performed on the 4 km domain. A 500 x 300 km grid box containing 24 trajectories was created in southern Wisconsin, an area that convection eventually entered. Backward trajectories were released from 800 mb at this location every 15 min, with each trajectory spanning 8 h. This analysis seeks to answer the question: For a box located in southern Wisconsin, how did the path of the air entering this area change, and how did the moisture along this path change? Fig. 8 depicts the initial and final values of  $q$  and  $rh$  as a function of trajectory ending time (using values computed from the average of all trajectories). Following the period of initial moistening of the pre-convective environment, the air over southern Wisconsin was insensitive to changes in  $q$  at the initial points of the trajectory. This phenomenon occurs because the colder air to the north in the box will become saturated with less moisture than the warmer downstream environment. This analysis enables us to quantitatively document the northward advance of moisture from the convection to the area of snowfall.

Trajectory analysis is also used to analyze the moisture characteristics of the CCB. A trajectory was found that passes through the precipitation just north of the strongest simulated reflectivities and subsequently enters the area of maximum snowfall (Fig. 9). Simulated reflectivity is shown for F2800, with the location of the air along the trajectory indicated by the boldened arrow. A cross section along the yellow line in Fig. 9a is presented in Fig. 9b. The air along the trajectory at F2800 is in a region

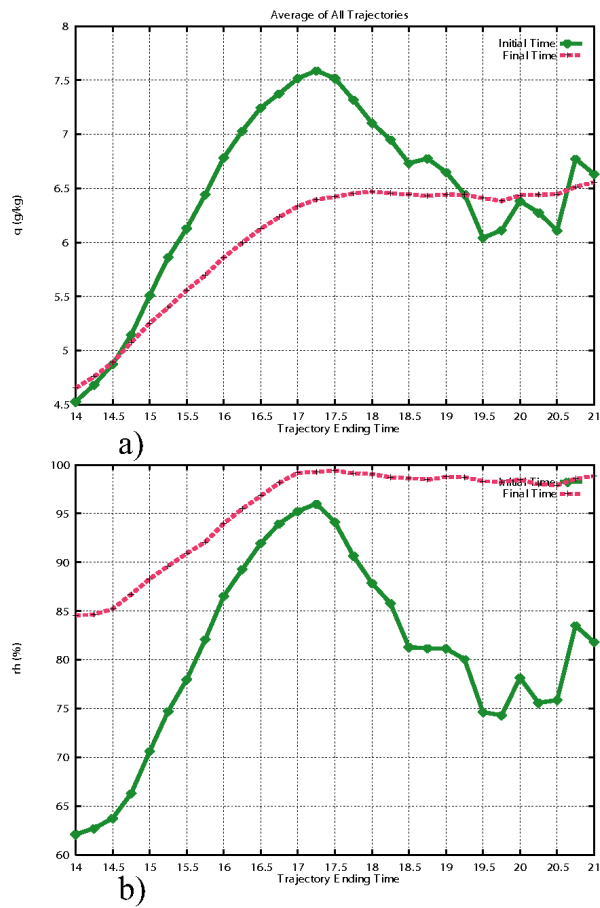


Figure 8: MM5 domain three evolution of moisture using the average of all trajectories, for (a)  $q$  ( $\text{g kg}^{-1}$ ) and (b)  $rh$  (%).

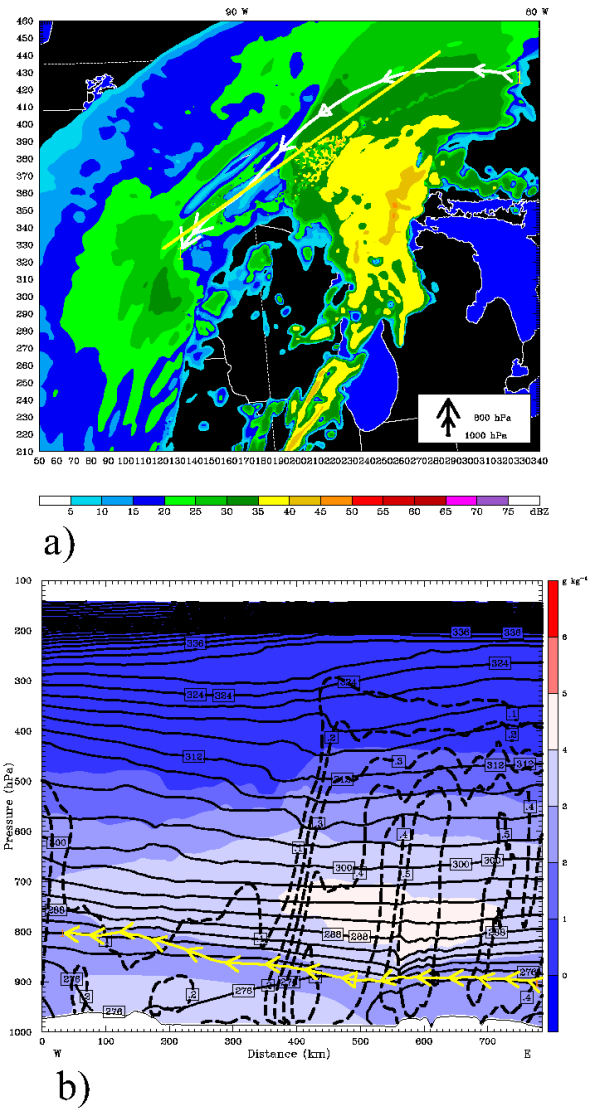


Figure 9: MM5 domain three (a) trajectory and reflectivity for 1600 UTC 23 Nov (F2800) and (b) cross section along line in (a), with  $q$  (shaded; scale at right),  $\theta$  (solid, 3 K), and total precipitation mixing ratio (dashed,  $0.1 \text{ g kg}^{-1}$ ).

of total precipitation mixing ratio of  $0.4 \text{ g kg}^{-1}$ , indicating precipitation was falling from the column encompassing this air. Based on this analysis, at least some air entering the banded snow region did pass through the precipitation just north of the convection. Therefore, from this analysis, there is no evidence that the convection reduced the moisture available for the snowfall. Also of importance, this trajectory is in the proper place and at the proper time to demonstrate the flow that was impacted by the flow induced by the convection.

## 7. CONCLUSIONS

Results of a PV budget demonstrate that significant low-level PV anomalies are generated diabatically, and are subsequently advected northward with the developing convection. Piecewise PV inversion of only the diabatically generated PV in the warm sector demonstrates that this PV contributed to the development of a diabatically induced surface low that was observed both in the model and in actuality. The inversion showed that the diabatically generated PV enhanced the CCB and associated moisture transport.

A moisture analysis along trajectories analyzed how the moisture associated with the developing convection advanced to the north. Low-level moisture was advected northward to an area between the convection and snowfall, and subsequently traveled from this area to provide a deep saturated layer even further north. Thus, saturation was maintained along the QLCS to the south and the snowfall to the north. Trajectories through the northern part of the convective area and into the region of snowfall show that any potential loss of condensate did not prevent snowfall from occurring.

## 8. ACKNOWLEDGEMENTS

Primary funding for this research is from NOAA-CSTAR under award number NA03-NWS4680019. The authors wish to thank Dr. Chris Davis for his assistance in this research.

\*

## REFERENCES

- Banacos, P. C., 2003: Short-range prediction of banded precipitation associated with deformation and frontogenesis forcing. *Preprints, Tenth Conf. on Mesoscale Processes*, Amer. Meteor. Soc., Portland, OR, CDROM, P1.7.
- Brennan, M. J., and G. M. Lackmann, 2005: The influence of incipient latent heat release on the precipitation distribution of the 24-25 january 2000 u.s. east coast cyclone. *Mon. Wea. Rev.*, **133**, 1913–1937.
- Cammag, J.-P., D. Keyser, G. M. Lackmann, and J. Molinari, 1994: Diabatic redistribution of potential vorticity accompanying the development of an outflow jet within a strong extratropical cyclone. *Proc. Int. Symp. on the Life Cycles of Extratropical Cyclones, Vol. II*, Geophysical Institute, University of Bergen, Bergen, Norway, 403-409.
- Davis, C. A., and K. A. Emanuel, 1991: Potential vorticity diagnostics of cyclogenesis. *Mon. Wea. Rev.*, **119**, 1929–1952.
- Grell, G. A., J. Dudhia, and D. R. Stauffer, 1995: A description of the fifth generation penn state/ncar mesoscale model (mm5). Tech. Rep. TN-398+STR, NCAR Technical Note.
- Jurewicz, M. L., and M. S. Evans, 2004: A comparison of two banded, heavy snowstorms with very different synoptic settings. *Wea. Forecasting*, **19**, 1011–1028.
- Lackmann, G. L., 2002: Cold-frontal potential vorticity maxima, the low-level jet, and moisture transport in extratropical cyclones. *Mon. Wea. Rev.*, **130**, 59–74.
- Moore, J. T., C. E. Graves, S. Ng, and J. L. Smith, 2005: A process-oriented methodology towards understanding the organization of an extensive mesoscale snow band: A diagnostic case study of 4-5 december 1999. *Wea. Forecasting*, **20**, 35–50.
- NCDC, 2006: Storm data. <http://www.ncdc.noaa.gov/oa/climate/sd/>.
- Novak, D. R., L. F. Bosart, D. Keyser, and J. S. Waldstreicher, 2004: An observational study of cold season-banded precipitation in northeast u.s. cyclones. *Wea. Forecasting*, **19**, 993–1010.
- Posselt, D. J., and J. E. Martin, 2004: The effect of latent heat release on the evolution of a warm occluded thermal structure. *Mon. Wea. Rev.*, **132**, 578–599.
- Raymond, D. J., 1992: Nonlinear balance and potential vorticity thinking at large rossby number. *Quart. J. R. Meteor. Soc.*, **118**, 987–1015.
- Stoelinga, M. T., 2005: A users' guide to rip version 4: A program for visualizing mesoscale model output. Available from <http://www.mmm.ucar.edu/mm5>.